

## Predictions of large events on a spring-block model

This article has been downloaded from IOPscience. Please scroll down to see the full text article.

1996 J. Phys. A: Math. Gen. 29 4445

(<http://iopscience.iop.org/0305-4470/29/15/016>)

View [the table of contents for this issue](#), or go to the [journal homepage](#) for more

Download details:

IP Address: 171.66.16.70

The article was downloaded on 02/06/2010 at 03:57

Please note that [terms and conditions apply](#).

## Predictions of large events on a spring-block model

Shu-dong Zhang<sup>†</sup>, Zu-qia Huang<sup>†</sup> and E-jiang Ding<sup>‡§||</sup>

<sup>†</sup> Institute of Low Energy Nuclear Physics, Beijing Normal University, Beijing 100875, People's Republic of China

<sup>‡</sup> CCAST (World Laboratory), PO Box 8730, Beijing 100080, People's Republic of China

<sup>§</sup> Institute of Low Energy Nuclear Physics, Beijing Normal University, Beijing 100875, People's Republic of China

<sup>||</sup> Institute of Theoretical Physics, Academia Sinica, Beijing 100080, People's Republic of China

Received 9 April 1996, in final form 20 May 1996

**Abstract.** We study the predictability of a theoretical model for earthquakes, using a pattern recognition algorithm similar to the CN and M8 algorithms known in seismology. The model, which is a stochastic spring-block model with both global correlation and local interaction, becomes more predictable as the strength of the global correlation or the local interaction is increased.

### 1. Introduction

Large earthquakes are disasters that cause losses of property and human lives. Unable to prevent earthquakes, people hope to predict large earthquakes so that the losses can be reduced to a minimum. In seismology, some empirical laws concerning the occurrence of earthquakes have been discovered, among which the best known one may be the Gutenberg–Richter relation [1], which expresses the earthquake frequency–energy relation as a power law. The G–R relation can take several different forms. Recently some authors showed, based on observational evidence, that the seismic moment is distributed according to the gamma distribution [2, 3] with probability density

$$\phi(M) \propto M^{-1-\beta} \exp(-M/M_{max}) \quad (1.1)$$

where  $M$  is the seismic moment and  $M_{max}$  is a ‘maximum moment’ for the distribution. Equation (1.1) is considered as a modified Gutenberg–Richter law. As in any other field of scientific research, the theoretical model also plays an important role in the study of earthquakes. The results obtained from some theoretical models may help to get some insights into the problem. The spring-block model is one of the theoretical models that have been used for the study of earthquakes and also served as a paradigm of the concept of self-organized criticality (SOC) [4].

In this paper we consider a spring-block model previously studied by Lu and Ding [5]. It was found in the Lu–Ding model that there is a scaling law

$$D(\Delta) \propto \Delta^{-\xi} \exp(-\Delta/\Delta_0) \quad (1.2)$$

between the slip size  $\Delta$  and its probability  $D(\Delta)$ , where  $\xi$  is a universal exponent with a value 1.5, and  $\Delta_0$  is a characteristic size of slip depending on the details of the system. The

slip size distribution in the Lu–Ding model is actually in the same form as the modified G–R relation (1.1). In this sense, the Lu–Ding spring-block model is a good model for an earthquake. In this paper, we shall not discuss too much the distribution of slip size, but only use this model to generate model earthquake catalogues. Applying a prediction algorithm to the model, we study the predictability of large events in the model.

## 2. The model

Detailed description of the Lu–Ding model can be found in the original papers of Lu and Ding [5, 6], herein we only give a brief description. The system consists of a total number  $N$  of blocks frictionally contacting a fixed carpet. At the beginning,  $N$  randomly chosen numbers,  $f_i$ 's, which are in the interval  $[0, f_t]$ , are assigned to each block as the pre-forces exerted on them, then the system is slowly driven so that the force exerted on each block increases uniformly with time, until one block, say the  $j$ th one, experiences a force  $f_j$ , which reaches the maximum friction  $f_t$ . Then the block will slip to a new position where the static friction between it and the fixed carpet becomes  $f_j^*$ . The slip of this block will increase the forces on other blocks. The system arranges itself according to the following dynamical rules:

$$\begin{cases} f_j \rightarrow f_j^* + \frac{\alpha}{(1+2\beta)N}u & f_j \geq f_t \\ f_{j\pm 1} \rightarrow f_{j\pm 1} + \frac{\alpha + N\beta}{(1+2\beta)N}u & i = j \pm 1 \\ f_i \rightarrow f_i + \frac{\alpha}{(1+2\beta)N}u & \text{otherwise} \end{cases} \quad (2.1)$$

where  $u = f_j - f_j^*$  is the decrease of the force on the  $j$ th block after its slipping, the parameter  $\alpha \in [0, 1]$  corresponds to the global correlation, and  $\beta \in [0, \infty)$  corresponds to local (nearest neighbour) interactions. The value of  $f_j^*$  is chosen randomly from the interval  $[0, f_t]$  through a given distribution function  $p(f)$  that is called the prestrain distribution.  $f_t$  is the maximum static friction between the carpet and the blocks, which is assumed to be the same for all blocks. After the rearrangement of the system according to the dynamical rules (2.1), there may be some other blocks, on which the resulting forces become larger than  $f_t$ . In this case the rules (2.1) must be used repeatedly until all the forces have values below  $f_t$  and thus no more blocks move. Before the system is further driven the total number  $\Delta$  of blocks which moved in a chain reaction is called the size of the slip. Notice that the total force  $F = \sum f_i$  may decrease after the rules (2.1) are used. The dissipation is proportional to

$$R = \frac{1 - \alpha}{1 + 2\beta}. \quad (2.2)$$

We define another quantity

$$C \equiv 1 - R = (\alpha + 2\beta)/(1 + 2\beta) \quad (2.3)$$

which will be referred to as the conservation level of the model. Here we emphasize that the terminology ‘conservation’ and ‘dissipation’ refers to the redistribution of forces.

Since the system of blocks is driven globally, the force added to each block will increase uniformly with time, thus the increase of force per block can be considered as a measure of the time. Hereafter in this paper we will take the increase of force per block as the time variable.

A real earthquake catalogue contains the position of the earthquake epicentre, the time and the magnitude of each earthquake which has occurred. Some modern catalogues even contain information about the focal mechanism of each earthquake [7–9]. In our studies, we use the Lu–Ding spring-block model to generate model catalogues, which record the slip events which occurred during the simulations of the model. The slip event in the model is considered as the analogue of an earthquake, and the size of the slip is analogous to the energy release of the earthquake.

### 3. Prediction algorithm

The prediction algorithm used in this paper is similar to the pattern-recognizing algorithm M8 and CN [10, 11]. Pepke *et al* [12, 13] have applied a similar method to some self-organizing systems such as Bak *et al*'s sandpile model [14], Olami *et al*'s spring-block model [15], etc. They also found a good precursory function, termed the size of active zone (SAZ) which, in their paper, is defined as the total number of blocks involved in the slip events during a period of time. Motivated by the M8 and CN algorithm as well as by Pepke *et al*'s work, we now apply a similar algorithm to the Lu–Ding model and investigate the predictability of the large slip events in this spring-block system.

To compare the effectiveness of the predictions based on different precursors, some normalization should be made to make the comparison meaningful. First, the length of the catalogue  $L$ , which is the total number of slip events recorded, should be the same for different predictions. Since we are studying a theoretical model, we can certainly let  $L$  be an arbitrary large number. In our prediction we chose  $L = 200\,000$ . Next, the minimum size  $\Delta^*$  of large events that are to be predicted is determined such that there are  $N_l$  slip events with size no less than  $\Delta^*$ :

$$N_l = \sum_{i=1}^L \theta(\Delta_i - \Delta^*) \quad (3.1)$$

where  $\Delta_i$  is the size of the  $i$ th slip event, and  $\theta(x)$  is the step function such that  $\theta(x) = 1$  for  $x \geq 0$  and  $\theta(x) = 0$  for  $x < 0$ . In our calculations, we chose  $N_l = 400$ .

The first precursory function we use in the prediction is called *activity*, which is defined as the total number of considerable events occurred within the time window  $W$  of the predictions,

$$A = \sum_{t \in W} \theta(\Delta_t - \underline{\Delta}) \quad (3.2)$$

where  $\underline{\Delta}$  is the minimum size of slip event that will be considered in the prediction; those events with size smaller than  $\underline{\Delta}$  will be ignored. In our prediction, we chose  $\underline{\Delta} = 2$ .

If  $A$  is a good precursory function, it should show systematic deviation from its usual values when a large event is about to occur. We find that in the Lu–Ding model, large events are preceded by a depression of the value of  $A$ , indicating that there is a relative quiescence before large events occur. The quiescence preceding large events is also present in the OFC model [12], but is not necessarily so for other models. This fact is similar to the present status of real earthquake predictions: some regions see a quiescence [16–18] preceding large earthquakes while other regions may experience frequent seismic activities [19, 20] before large earthquakes.

We set a threshold value for  $A$ , say  $A_c$ . Then we move the time window along the catalogue and monitor the value of  $A$  all the time. Whenever  $A \leq A_c$ , we turn TIP (time

of increased probability) on, warning that a large event may occur at any moment. Once  $A$  returns to  $A > A_c$ , the TIP alarm will be turned off. After the catalogue is scanned by the time window, there will be some time intervals that are issued as TIP. A large event occurring during TIP is considered as being successfully predicted, while a large event occurring without TIP alarm is *missed* by the prediction. A period declared as TIP but without large events occurring is a false alarm. If we let  $p_1$  be the percentage of large events that have been successfully predicted:

$$p_1 = \frac{\text{number of large events successfully predicted}}{\text{total number of large events to be predicted}} \quad (3.3)$$

and  $p_2$  be the fraction of the total time that has been declared as TIP:

$$p_2 = \frac{\text{time issued as TIP}}{\text{total time}} \quad (3.4)$$

then for every given threshold value  $A_c$  we get a point  $(p_1, p_2)$  in a plot of  $p_1$  versus  $p_2$ . Varying  $A_c$  we get a curve for prediction, which is called the *success curve* [21]. The effectiveness of the prediction then can be evaluated by the quantity  $S = p_1/p_2$ . If  $S > 1$ , it suggests that the prediction is meaningful since it is better than a random prediction. Random prediction is based on no information about the system but only turns on and off TIP randomly. For the random prediction, in a statistical sense, a fraction of alarm time will catch the same fraction of large events, i.e.  $p_1 = p_2$ . So the success curve obtained from the random prediction is a diagonal line in the  $(p_1, p_2)$  plot. We made a random prediction on one of the model catalogues. The result shown in figure 1 confirms the above consideration. So any prediction whose success curve lies above the diagonal line is better than the random prediction and thus is meaningful. The success curve based on the precursor function  $A$  is shown in the lowest broken curve in figure 2. Since this curve is above the random prediction (the diagonal line) we consider the prediction based on this precursory function meaningful. But it is not very robust because this curve is only slightly better than the random prediction.

The second precursory function we use can be called the *total released energy* (TRE) of the events within the time window, which is the sum of the sizes of all the considerable events,

$$E = \sum_{i \in W} \Delta_i \theta(\Delta_i - \underline{\Delta}) \quad (3.5)$$

where  $\Delta_i$  is the size of an individual event  $i$ , and  $\theta(x)$  is the step function. For this precursory function, we turn TIP on when  $E \leq E_c$ , where  $E_c$  is a threshold value that will be varied to get the success curve. We find that this precursor works much better than the activity  $A$ , probably because it incorporates more information into the prediction than the activity  $A$  does. Figure 2 also shows the results based on this precursor. With  $E$  as precursor, when 30% of the time is declared as TIP, about 80% of large events can be predicted.

In order to improve the prediction effectiveness further, we consider in the Lu–Ding spring-block model the total force  $F$  on the system, which reads

$$F = \sum_{i=1}^N f_i. \quad (3.6)$$

Notice that the precursory function  $F$  is only a function of time, unlike the activity  $A$  and the total released energy  $E$ , which are functions of a time window  $W$ . For this precursory

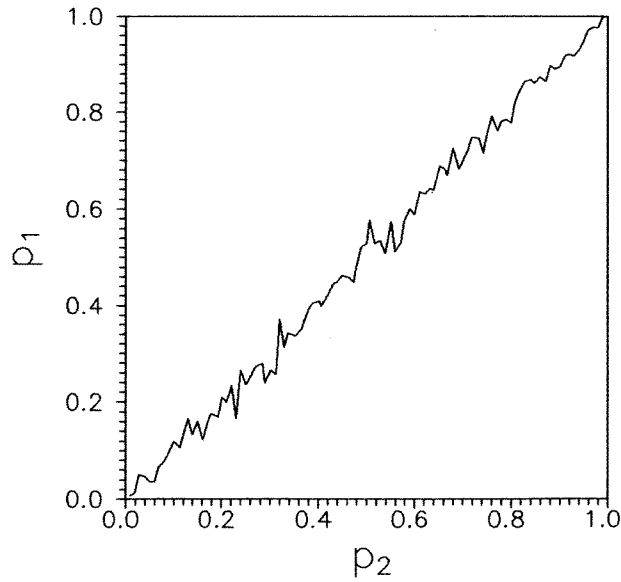


**Figure 1.** The success curve for a random prediction. In principle, this should be a diagonal line in the  $p_1$  versus  $p_2$  plot. In all the following figures, the diagonal line is also plotted for comparison.

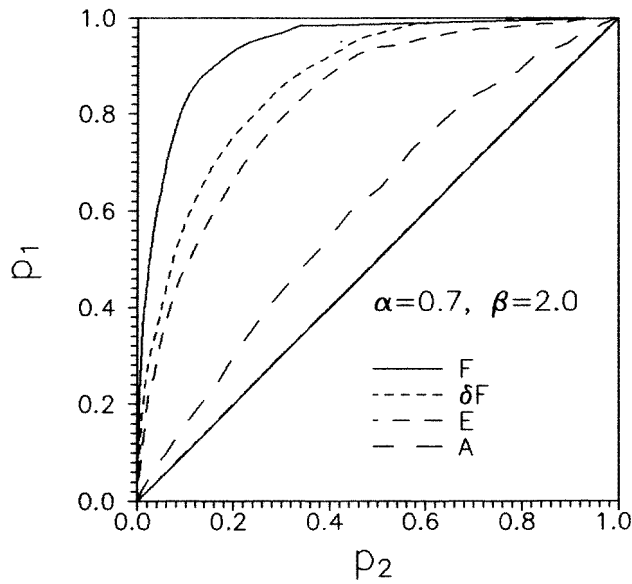


**Figure 2.** The success curves for the predictions with  $A$ ,  $E$ ,  $F$ , and  $\delta F$  as precursors. The total force  $F$  has the best performance. In this figure, the number of blocks  $N = 250$ , the parameters  $\alpha = 0.7$ ,  $\beta = 2$ . The conservation  $C = 0.94$ . The time interval of the time window is 0.1 net force added per block, the length of the model catalogue  $L = 200\,000$ , the number of large events to be predicted  $N_l = 400$ , the minimum size of event to be considered  $\underline{\Delta} = 2$ .

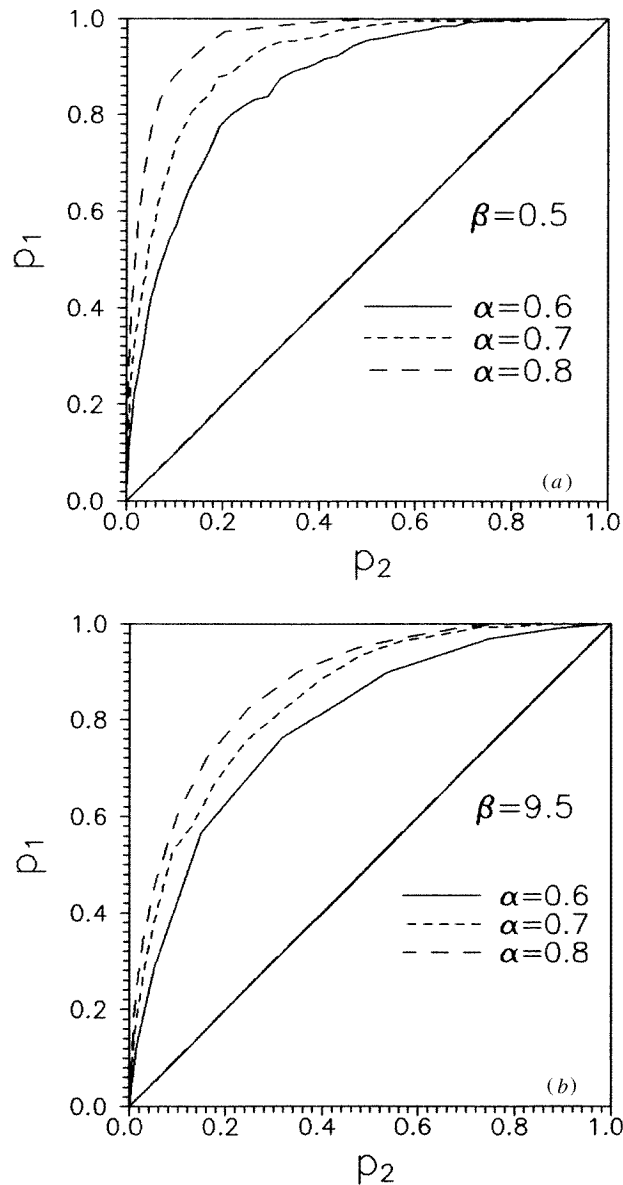


**Figure 3.** When the value of  $\beta$  is fixed, a larger  $\alpha$  gives a more predictable Lu–Ding model. (a) The success curves based on the precursory function  $F$  for the cases  $\beta = 0.5$ . (b) Using the total released energy  $E$  as precursor.  $\beta = 9.5$ .

function, the TIP is turned on when  $F \geq F_c$ , where  $F_c$  is a given threshold in the prediction. Using  $F$  as the precursory function, we can successfully predict nearly 90% of large events with only 15% of time issued as TIP alarm (for the case shown in figure 2).

Although the total force  $F$  is a relatively good precursory function for this theoretical model, it suffers from the drawback that the measurement of this quantity in practice is difficult and indirect. One difficulty is the determination of the zero point of the stress or strain in rocks. It is the increment of stresses or strains that can be measured with

certain electronic or mechanical techniques. To make our discussion more practical, we now consider another precursory function, the increment of the force within a time window, which is defined as

$$\delta F = F(t + \delta t) - F(t) \quad (3.7)$$

where  $\delta t$  is the width of the time window  $W$ . In the prediction, we turn TIP on when  $\delta F$  becomes larger than a given threshold  $\delta F^c$ . The results of prediction based on  $\delta F$  are also shown in figure 2. With this precursory function, when about 25% of the time is issued as TIP, more than 80% of large events can be successfully predicted. The performance of  $\delta F$ , as expected, is not as good as that of  $F$ , but is slightly better than that of the precursory function  $E$ .

#### 4. The effects of the global and local interactions on the predictability of the model

First, we study the effects of the global correlation on the predictability of the model. In doing so, we fix the value of  $\beta$  and vary  $\alpha$ . Typical results are shown in figure 3, from which we see that for given  $\beta$  the model becomes more predictable as  $\alpha$  is increased. Figure 3(a) shows the results for the cases  $\beta = 0.5$ ; the three success curves are for  $\alpha = 0.6, 0.7$  and  $0.8$ , respectively. When  $\alpha = 0.6$ , about 20% of the time needs to be declared as TIP in order to catch 80% of large slip events; when  $\alpha = 0.7$ , the fraction of time that needs to be TIP is reduced to 13% to catch the same amount of large events. As  $\alpha$  is increased to  $0.9$ , the prediction becomes better. We see that only 5% of the time needs to be TIP alarm in order to catch 80% of large events. The result that larger  $\alpha$  gives a better prediction performance is also true for other values of  $\beta$  and for other precursors. For examples, we show in figure 3(b) the results for the case  $\beta = 9.5$  with  $E$  as the precursory function.

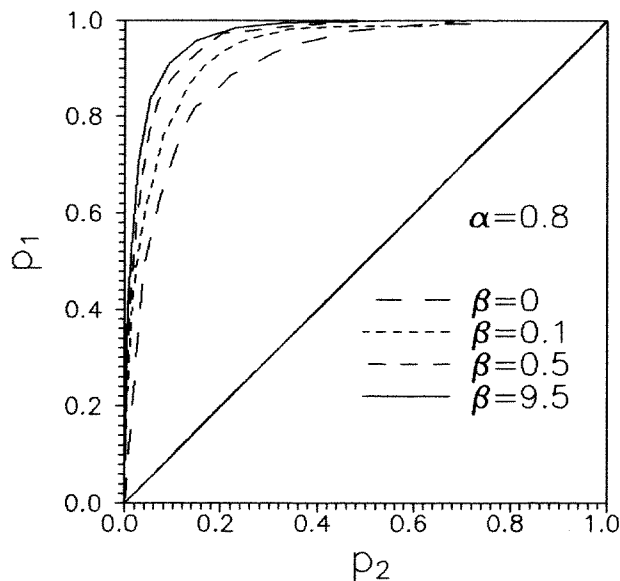


**Figure 4.** The effect of local interaction on the predictability of the Lu–Ding model. A greater  $\beta$  gives a higher predictability. The four success curves are based on the precursory function  $F$ .



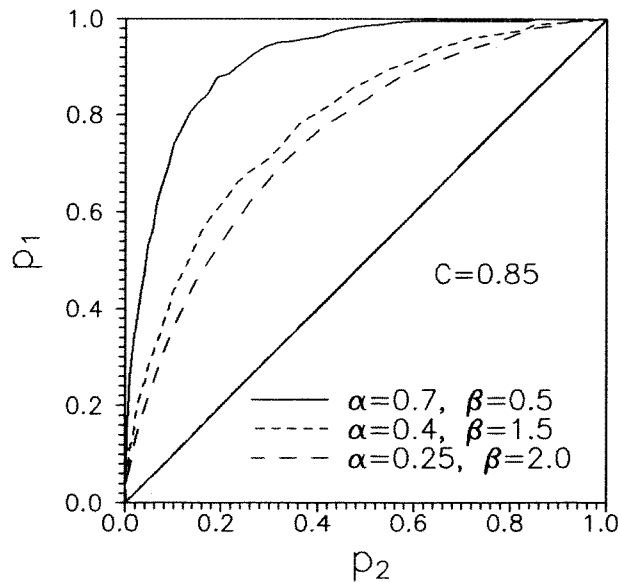


**Figure 5.** For different  $\alpha$  and  $\beta$  but fixed  $C$ , the predictability of the Lu-Ding model is mainly determined by the strength of global correlation.

Next, we investigate the effect of the local interaction on the predictability of the model. We found that when  $\alpha$  is fixed, a larger  $\beta$  gives a better prediction performance. In figure 4, we show the results for the case  $\alpha = 0.8$ ,  $\beta = 0, 0.1, 0.5$  and  $9.5$ . The success curve for  $\beta = 9.5$  is the best one among the four curves shown in this figure. We note that if  $\beta$  becomes larger than  $9.5$ , the predictions will not improve too much, which means that for a given  $\alpha$  there is a saturation value of  $\beta$  beyond which the prediction effectiveness no longer increases.

One may ask whether the conservation level  $C$  uniquely determines the effectiveness of the prediction. The answer is ‘no’. Actually, we show in figure 5 that the prediction effectiveness with different  $\alpha$  and  $\beta$  is quite different, although the conservation level is fixed at  $C = 0.85$ . Besides, calculations show that the effectiveness of the success curves is mainly determined by the parameter  $\alpha$ .

## 5. Stochastic versus deterministic

When  $\alpha = 0$  the Lu-Ding model reduces to a complete locally interacted model. In this case, a larger  $\beta$  still gives a more predictable model than a smaller  $\beta$  (see figure 6(a)).

Here we recall the prediction results for the OFC spring-block model [15]. The OFC model also has an adjustable parameter serving as the conservation level. The effect of the conservation level on the predictability of the OFC model was reported by Pepke and Carlson [12]. Their typical results suggested that, in the OFC spring-block model, as the conservation level is increased the large events become less predictable (with SAZ as the precursor). We present in figure 6(b) the prediction curves for the OFC model using the total force  $F$  as the precursory function. Figure 6(b) clearly shows that the increase of the conservation level will reduce the predictability of the OFC model. This result for the OFC model is in sharp contrast to that of the Lu-Ding model (see figure 6(a)). How does this

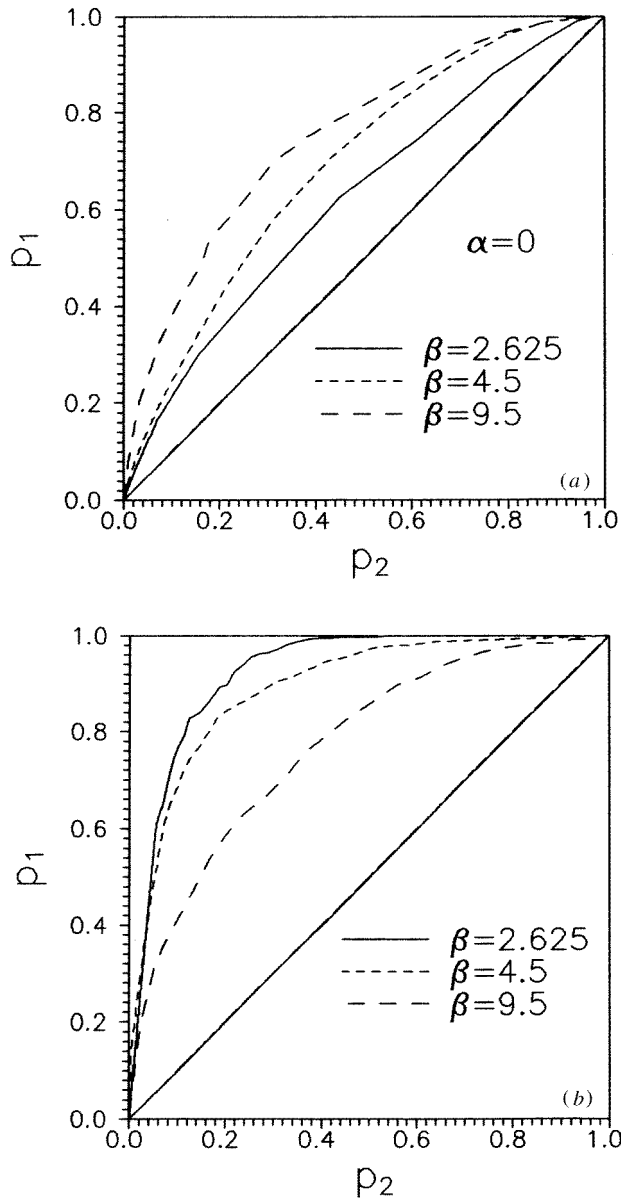


**Figure 6.** Comparisons between the OFC model and the 2D Lu-Ding model. In this figure for both the OFC model and the 2D Lu-Ding model, the numbers of blocks in the system are  $N = 20 \times 20 = 400$ . (a) For the 2D Lu-Ding model, with  $E$  as precursory function. Larger  $\beta$  makes the Lu-Ding model more predictable. (b) For the OFC model, with  $F$  as precursory function. Larger  $\beta$  (higher conservation level) makes the OFC model less predictable.

happen? Let us look back into the major differences between the two models.

For comparison purposes we now generalize the Lu-Ding model to its two-dimensional

case. It is straightforward to get the dynamical rules of the 2D Lu–Ding model,

$$\left\{ \begin{array}{l} f_{i,j} \rightarrow f_{i,j}^* + \frac{\alpha}{(1+2\beta)N} u \quad f_{i,j} \geq f_t \\ f_{i\pm 1,j} \rightarrow f_{i\pm 1,j} + \frac{\alpha}{(1+2\beta)N} u + \frac{\beta}{2(1+2\beta)N} u \\ f_{i,j\pm 1} \rightarrow f_{i,j\pm 1} + \frac{\alpha}{(1+2\beta)N} u + \frac{\beta}{2(1+2\beta)N} u \\ f_{m,n} \rightarrow f_{m,n} + \frac{\alpha}{(1+2\beta)N} u \quad m \neq i \pm 1 \quad n \neq j \pm 1 \end{array} \right. \quad (5.1)$$

where  $u = f_{i,j} - f_{i,j}^*$ .

On the other hand, the dynamical rules for the OFC model are

$$\left\{ \begin{array}{l} f_{i,j} \rightarrow 0 \quad f_{i,j} \geq f_t \\ f_{i\pm 1,j} \rightarrow f_{i\pm 1,j} + \frac{\beta}{2(1+2\beta)N} u \\ f_{i,j\pm 1} \rightarrow f_{i,j\pm 1} + \frac{\beta}{2(1+2\beta)N} u \\ f_{m,n} \rightarrow f_{m,n} \quad m \neq i \pm 1 \quad n \neq j \pm 1 \end{array} \right. \quad (5.2)$$

where  $u = f_{i,j}$ .

If we take  $\alpha = 0$  in the 2D Lu–Ding model, the only difference between the two models is the value of  $f_{i,j}^*$ . In the Lu–Ding model,  $f_{i,j}^*$  is chosen randomly in the interval  $[0, f_t]$ . In this sense the Lu–Ding model is a stochastic model. In the OFC model,  $f_{i,j}^*$  is uniquely chosen to be  $f_{i,j}^* = 0$ , so the OFC model is a deterministic model. The only randomness involved in the OFC model is the randomly assigned pre-force on each block. It is the presence of the randomness that makes the behaviour of the Lu–Ding model different from that of the OFC model. We also find that because of the absence of randomness in the OFC model the one-dimensional OFC model has only a trivial periodic behaviour, and does not exhibit SOC. On the other hand, the Lu–Ding model shows a complicated behaviour even in its one-dimensional version.

## 6. Summary and discussions

In this paper we have applied a pattern-recognizing algorithm to predict the large events in the Lu–Ding model. Four kinds of precursors are used, among which the most effective is the total force  $F$ . The global interaction and local interaction both affect the results of prediction. For the Lu–Ding model, it becomes more predictable as  $\alpha$  and  $\beta$  are increased. Especially, we find in the case when the global interaction is turned off that the Lu–Ding model becomes more predictable as the conservation level is increased, which is in sharp contrast to the results for the OFC model.

We notice that some authors have suggested that the events in a self-organizing critical system might be unpredictable [22]. Our predictions on the OFC model and the Lu–Ding model point to the opposite direction of that argumentation. All of the predictions performed are better than the random prediction. The relatively better performance by  $F$  and  $\delta F$  suggests that to make more effective predictions, more information about the system should be obtained. Recently, de Sousa Viera and Lichtenberg showed that some SOC models might be chaotic, in the sense that the largest Liapunov exponent (LLE) of

these systems is greater than zero [23], which certainly should affect the predictability. The spring-block system studied by de Sousa Viera and Lichtenberg was a deterministic model. For earthquake modelling, we prefer stochastic spring-block models such as the Lu–Ding model. In fact, the earthquake occurrence is characterized by extreme randomness, and the stochastic nature of seismicity is not reducible by more numerous or more accurate measurements [3].

### Acknowledgments

This work is supported by the National Nature Science Foundation, the National Basic Research Project ‘Nonlinear Science’ and the State Educational Commission through the Foundation of Doctoral Training.

### References

- [1] Gutenberg B and Richter 1954 *Seismicity of the Earth and Related Phenomena* (Princeton, NJ: Princeton University Press)
- [2] Kagan Y Y 1991 *Geophys. J. Int.* **106** 123
- [3] Kagan Y Y 1994 *Physica* **77D** 160
- [4] Bak P and Tang C 1989 *J. Geophys. Res.* **94** 15 535
- [5] Lu Y N and Ding E J 1993 *Phys. Rev. E* **48** R21
- [6] Ding E J and Lu Y N 1993 *Phys. Rev. Lett.* **70** 3627
- [7] Sipkin S A and Needham R E 1992 *Phys. Earth Planet. Inter.* **70** 16
- [8] Dziewonski A M, Ekstrom G and Salganik M P 1993 *Phys. Earth Planet. Inter.* **77** 143
- [9] US Geological Survey, Preliminary determination of epicenters, Monthly Listings, US Dep. of Inter., Natl Earthquakes Inf. Cent., Denver, Jan. 1993.
- [10] Keilis-Borok V I and Rotwain I M 1990 *Phys. Earth Planetary Inter.* **61** 57
- [11] Keilis-Borok V I and Kossobokov V G 1990 *Phys. Earth Planetary Inter.* **61** 73
- [12] Pepke S L and Carlson J M 1994 *Phys. Rev. E* **50** 236
- [13] Pepke S L, Carlson J M and Shaw B E 1994 *J. Geophys. Res.* **99** 6769
- [14] Bak P, Tang C and Wiesenfeld K 1987 *Phys. Rev. Lett.* **59** 381; 1988 *Phys. Rev. A* **38** 364
- [15] Olami Z, Feder H and Christensen K 1992 *Phys. Rev. Lett.* **68** 1244  
Christensen K and Olami Z 1992 *Phys. Rev. A* **46** 1829
- [16] Scholz C H 1988 *Pure Appl. Geophys.* **126** 701
- [17] Myss M and Haberman R E 1988 *Pure Appl. Geophys.* **126** 319
- [18] Schreider S Y 1990 *Phys. Earth Planetary Inter.* **61** 113
- [19] Keilis-Borok V I 1990 *Rev. Geophys.* **28** 19
- [20] Sykes L R and Janume S C 1990 *Nature* **348** 595
- [21] Mochan G M 1991 *Tectonophysics* **193** 267
- [22] Barriere B and Turcotte D L 1994 *Phys. Rev. E* **49** 1151
- [23] de Sousa Viera M and Lichtenberg A J 1996 *Phys. Rev. E* **53** 1441